Journal Pre-proof

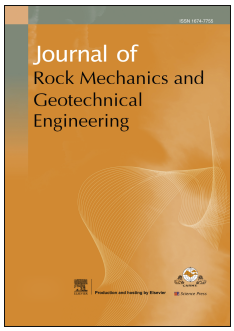

Impact of flow direction on suffusion of sand-clay mixtures under variably saturated conditions

Yerim Yang, Hangseok Choi, Jooho Lee, Yongjoon Choe, Jongmuk Won

PII: S1674-7755(24)00390-1

DOI: https://doi.org/10.1016/j.jrmge.2024.05.038

Reference: JRMGE 1701

To appear in: *Journal of Rock Mechanics and Geotechnical Engineering*

Received Date: 6 January 2024

Revised Date: 2 April 2024

Accepted Date: 28 May 2024

Please cite this article as: Yang Y, Choi H, Lee J, Choe Y, Won J, Impact of flow direction on suffusion of sand-clay mixtures under variably saturated conditions, *Journal of Rock Mechanics and Geotechnical Engineering*, https://doi.org/10.1016/j.jrmge.2024.05.038.

Impact of flow direction on suffusion of sand-clay mixtures under variably saturated conditions

Yerim Yang [a], Hangseok Choi [a,*], Jooho Lee [a], Yongjoon Choe [b], Jongmuk Won [c,**]

[a] School of Civil, Environmental and Architectural Engineering, Korea University, Anam-dong 5 ga, Seoul, 136-713, South Korea
[b] School of Civil and Environmental Engineering, Georgia Institute of Technology, Atlanta, GA 30332-0355, USA
[c] Department of Civil, Urban, Earth, and Environmental Engineering, Ulsan National Institute of Science and Technology (UNIST), UNIST-gil 50, Ulju-gun, Ulsan, 44919, South Korea

*Corresponding author.
**Corresponding author.
E-mail addresses: hchoi2@korea.ac.kr (Hangseok Choi), jwon@unist.ac.kr (Jongmuk Won)

ABSTRACT: Suffusion is the process defined as the migration of relatively small soil particles through the pores of a soil matrix composed of relatively large particles, driven by substantial hydrodynamic forces and weak attraction energies. This study investigates the influence of flow direction (upward and downward) on suffusion induced by interaction energies in sand-clay mixtures under both saturated and unsaturated conditions. The impact of clay mineralogy (kaolinite, illite, and montmorillonite), sand-grain size, and ionic concentration (IC) gradient were discussed based on the observed breakthrough curves (BTCs) and relative saturation rate (S_r) during injection (particularly for unsaturated conditions). Under saturated conditions, higher susceptibility to suffusion was observed in sand-kaolinite and sand-illite mixtures under downward flow compared to upward flow, whereas the suffusion of montmorillonite was more significant under upward flow than under downward flow. In contrast, for unsaturated conditions, more substantial suffusion of kaolinite and illite particles occurred under upward flow compared to downward flow, whereas the opposite trend was observed in sand-montmorillonite mixtures. In addition, the impact of sand-grain size (or the size ratio between sand and clay) on the suffusion of kaolinite and illite under unsaturated conditions suggests a reduced size ratio that leads to relatively significant suffusion under downward flow compared to upward flow. The findings presented in this study contribute to a comprehensive understanding of the influence of flow direction on suffusion in sand-clay mixtures under both saturated and unsaturated conditions.
Keywords: Suffusion; Breakthrough curve (BTC); Sand-clay mixture; Saturated soil; Unsaturated soil; Ionic concentration (IC); Flow direction; Clay mineralogy

1. Introduction

Suffusion is one of the main internal erosion mechanisms of the soil matrix, which leads to structural instability of dams, dikes, and levees (Fell and Fry, 2007). During the suffusion process, relatively fine particles subjected to seepage forces migrate through the pore space of coarse particles (Rochim et al., 2017; Benamar et al., 2019; Kodieh et al., 2021). Because the loss of fine particles increases the porosity within the soil matrix, the suffusion can decrease the strength and stiffness of soils (Chang et al., 2014; Ke and Takahashi, 2014; Xu et al., 2021). Therefore, a comprehensive understanding of suffusion is needed for the long-term sustainability of earthen structures.

The susceptibility of suffusion can be influenced by many geometric factors (e.g. particle size distribution and particle shape) and hydraulic factors (e.g. hydraulic gradient and chemical properties of the pore water) (Zhang et al., 2019). Among those factors, hydraulic gradient (or hydrodynamic forces) has been considered the most critical factor inducing suffusion, which has been investigated in many previous studies that have focused on the hydraulic-induced suffusion for coarse-grained gap-graded soils as a function of size distribution, porosity, and hydraulic conductivity (Liang et al., 2017; Rochim et al., 2017; Rasheed et al., 2018; Israr and Indraratna, 2019; Liu et al., 2020; Chen et al., 2021). Apart from the hydraulic gradient, the increase in repulsion energy between coarse and fine particles can also induce suffusion, particularly when the fine particles are clay minerals (Choe et al., 2022; Won, 2022; Won et al., 2023). The decrease in ionic concentration (IC) increases the repulsion energy, hence increases the susceptibility of suffusion in coarse-fine mixtures (Blume et al., 2005; Benamar, 2014; Chetti et al., 2016; Choe et al., 2022; Won et al., 2023). Therefore, it is necessary to incorporate the solution chemistry of coarse-fine mixtures at given hydraulic conditions to assess the suffusion of clay particles.

Many previous studies have investigated the flow direction or gravity effect on the suffusion of coarse-grained gap-graded soils in saturated conditions using numerical modelings (Zhou et al., 2020; Ma et al., 2021; Xiong et al., 2021; Liu et al., 2023). While the movement of clay particles in the aqueous phase may not be significantly affected by flow direction due to their small particle sizes, their high specific gravity causes the settling of these clay particles during they move through the sand matrix (Imai, 1980; McDowell-Boyer et al., 1986; Kotlyar, 1998; Gao, 2007). In addition, the aggregation of clay particles can form clay clusters that are even larger than individual clay particles (Palomino and Santamarina, 2005; Reichert et al., 2009; Sutherland et al., 2015), the flow direction may affect the suffusion of sand-clay mixtures, which can be inferred from the different suffusion characteristics of fine-grained soils as a function of flow direction (Basha and Culligan, 2010; Chrysikopoulos and Syngouna, 2014; Jiang et al., 2016; Pachideh and Majdeddin Mir Mohammad Hosseini, 2019; Tu et al., 2022).

The abovementioned studies have investigated suffusion under initially saturated conditions. However, suffusion can occur under unsaturated conditions due to rain infiltration and fluctuations in the water table (Collins and Znidarcic, 2004; Tsai and Chen, 2010; Lei et al., 2017, 2020; Zhang et al., 2019, 2023; Deng et al., 2024). Under unsaturated conditions, varying degree of saturation within the soil matrix under different flow directions is anticipated. Since unsaturated soil properties (e.g. matric suction and hydraulic conductivity) are a function of water content (Hassanizadeh et al., 1997; Lu and Likos, 2004, 2006; Fredlund et al., 2012), the suffusion of unsaturated soils can be highly affected by flow direction because water content varies depending on flow direction. This is particularly relevant in scenarios where the detachment of fine particles is prevalent. However, the impact of flow direction on suffusion of clay-containing soils under unsaturated conditions has not been documented to date. Therefore, the objective of this study is to investigate the impact of flow direction on interaction energy-induced suffusion of sand-clay mixtures under saturated and unsaturated conditions. The laboratory soil-column experiments were designed to simulate upward and downward flows through sand-clay mixtures under two IC gradients (gradual and stepwise decrease in IC). The impact of flow direction, saturation state, clay mineralogy, and sand-grain size was discussed through observed breakthrough curves (BTCs) and relative saturation rate (S_r) during the injection.

2. Materials and methods

2.1. Materials

Three types of clay (kaolinite, illite, and montmorillonite) and three types of sand (K3, K5, and K6) were selected to investigate the impact of the clay mineralogy and size ratio on suffusion in sand-clay mixtures. The mineralogical and chemical composition of the specimens used in this study were analyzed using X-ray diffraction (XRD) (step size (2θ) = 0.017°, X-ray voltage = 40 kV, and X-ray current = 30 mA) and X-ray fluorescence (XRF), as presented in Fig. 1 and Table 1, respectively. The XRD results of the clay (Fig. 1) revealed that the three clays consisted predominantly of kaolinite, illite, and montmorillonite, respectively. In addition, all sand specimens (from Kangwon Province, South Korea) used in this study have a silica (SiO_2) content greater than 74% (Table 1).

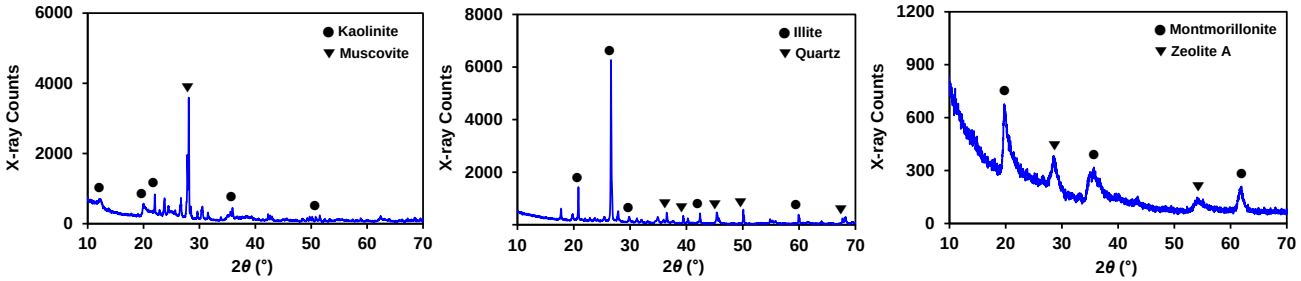

(a) (b) (c)

Fig. 1. XRD patterns of (a) kaolinite, (b) illite, and (c) montmorillonite used in this study (analyzed by the Korea Basic Science Institute).

Table 1
X-ray fluorescence (XRF) results of the clay and sand used in this study (analyzed by the Korea Basic Science Institute).

Component	Mass percentage (%)					
	Kaolinite	Illite	Montmorillonite	K3	K5	K6
SiO_2	51.6	60.7	50.8	82.6	74.6	74.1
Al_2O_3	33.8	20.2	15.7	3.06	10.9	12.2
CaO	9.16	0.175	3.14	9.32	0.779	1.08
Fe_2O_3	2.81	9.35	22.1	0.758	1.79	1.6
K_2O	0.855	6.97	0.247	1.7	9.27	8.1
Na_2O	0.85	0.471	1.94	0.044	1.73	3.11
MgO	0.38	0.572	2.6	1.74	0.05	0.013
TiO_2	0.285	1.11	1.45	0.248	0.072	0.013
P_2O_5	0.114	0.159	0.476	0.239	0.224	0.012
SrO	0.09	0.017	0.064			
MnO	0.026	0.129	0.084		0.167	0.127
CuO	0.02		0.055	0.029	0.022	
Cr_2O_3				0.09	0.08	
SO_3					0.053	
Rb_2O				0.01	0.175	
ZrO_2				0.161	0.019	
WO_3				0.049		
PbO					0.03	
SrO					0.019	
Ga_2O_3					0.014	
Nb_2O_5					0.01	
ZnO	0.011	0.02	0.056		0.049	

The physical properties of the clay and sand were evaluated using ASTM standards as summarized in Table 2. To evaluate the specific gravity (G_s), the volumes of soil specimens of known weights were measured by immersing them in a pycnometer filled with water (ASTM D854, 1999). The maximum and minimum void ratios of the sand specimens (e_{max} and e_{min}) were determined using the funnel deposition method (ASTM D4253, 1996) and the vibrating table method (ASTM D4254, 2006). The particle size distributions (PSDs) demonstrated in Fig. 2 were obtained through hydrometer tests for clay and sieve analysis for sand (ASTM D422, 2007). The median grain size (d_{50}) and the uniformity coefficient (C_u) were evaluated based on the obtained PSDs. Based on the d_{50} values evaluated from the PSDs, the size ratio (SR) between sand and clay was defined as follows:

$$SR = d_{50(\text{sand})}/d_{50(\text{clay})} \quad (1)$$

In addition, the low C_u (< 1.5) of the sands (Table 2) demonstrated relatively uniform particle sizes of sand used in this study. The pictures of the sand and clay are presented in Fig. 3.

Table 2
Properties of clay and sand used in the experiments.

Parameter	Testing method	K3	K5	K6	Kaolinite	Illite	Montmorillonite
G_s	ASTM D854	2.65	2.65	2.65	2.47	2.71	2.36
e_{max}	ASTM D4253	0.845	0.972	1.085			
e_{min}	ASTM D4254	0.728	0.735	0.791			
d_{50} (mm)	ASTM D422	1.7	0.83	0.47	10.5×10^{-3}	9×10^{-3}	1×10^{-3}
C_u		1.45	1.45	1.48	11.87	6.43	
n_{sand}		0.433	0.446	0.468			
$\gamma_{d\ clay\ 3\%}$		1.591	1.544	1.544			

Note: G_s = specific gravity; e_{max} = maximum void ratio; e_{min} = minimum void ratio; d_{50} = median grain size; C_u = uniformity coefficient; n_{sand} = porosity of sand corresponding to a relative density of 70%; $\gamma_{d\ clay\ 3\%}$ = dry unit weight of 3% sand-clay mixtures.

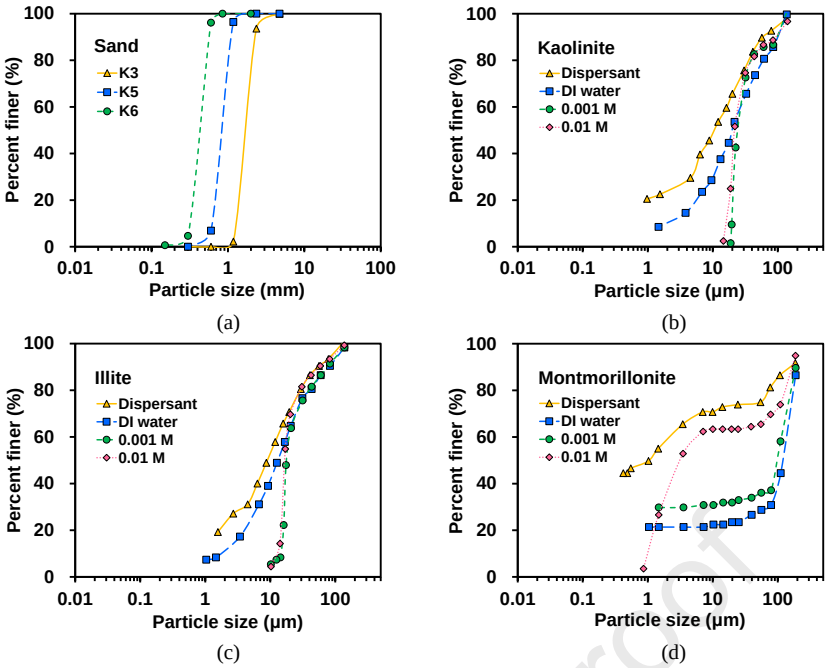

Fig. 2. Particle size distributions (PSDs) of (a) K3, K5, and K6 sands (sieve analysis), and particle size distributions (PSDs) of (b) kaolinite, (c) illite, and (d) montmorillonite under varying conditions, with addition of dispersant, 0 (DI water), 0.001, and 0.01 M of NaCl solution (hydrometer tests).

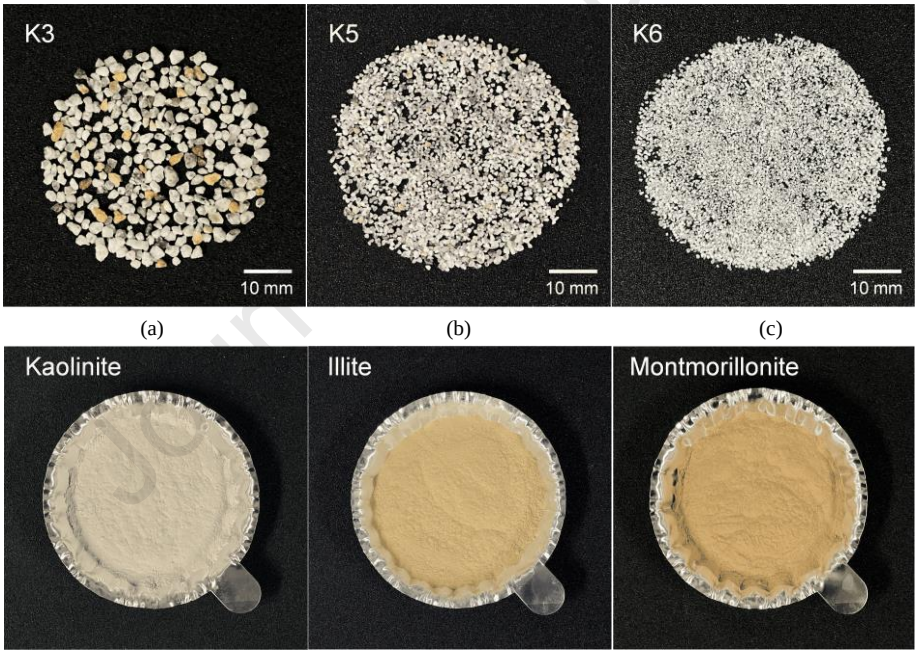

Fig. 3. Pictures of the sand ((a) K3, (b) K5, and (c) K6) and clay ((d) kaolinite, (e) illite, and (f) montmorillonite) used in the experiments.

2.2. Soil column test

The sand specimens were washed and placed in a sonicator bath (frequency = 40 kHz) to eliminate impurities until the turbidity of the supernatant reached less than 10 nephelometric turbidity unit (NTU). The sand was then oven-dried and mixed with clay at a clay content of 3% by weight in an airtight container for 0.5 h to prepare a homogeneous sand-clay mixture corresponding to a relative density of 70%. This mixture was then placed into an acrylic column (diameter = 5.08 cm, height = 15.24 cm). The low clay content of 3% was selected specifically to investigate suffusion induced by detachment solely at the sand-clay interfaces. Higher clay contents, exceeding 3%, may lead to detachment not only at the sand-clay interfaces but also at the clay-clay interfaces. For the saturated experimental conditions, the wet pluviation method was applied to ensure an initial fully saturated condition (0.01 M NaCl solution) of sand-clay mixtures without segregation. The minimum segregation with a semi-homogeneous state of sand-clay mixtures was obtained by the gradual increase in the water level slightly higher than the sample height during the wet pluviation method. For unsaturated conditions, a dry sand-clay mixture was placed into the column without any saturation process to form the initial dry conditions.

An IC-controlled NaCl solution (decrease in IC from 0.01 to 0 M) was injected into the soil column to induce the interaction energy-induced suffusion of sand-clay mixtures. To investigate the impact of flow direction, upward and downward flow directions were selected by injecting the solution at the bottom (upward flow) and the top of the column (downward flow). At a constant flow rate of 15 mL/min, the injection was terminated when the injection volume reached 15 pore volumes (PVs). The volume injected for 15 PVs amounted to 1932.8, 2012.4, and 2012.7 mL for K3, K5, and K6 sands, respectively (namely, the single pore volume of the sand matrix was 128.86, 134.16, and 134.18 mL for K3, K5, and K6 sands, respectively). In addition, the IC of the solution was decreased with two IC reduction scenarios of gradual decrease (GD) and stepwise decrease (SD) to investigate the impact of IC gradient on suffusion. The IC rapidly decreased from 0.01 to 0.001 M at PV = 5 and from 0.001 to 0 at PV = 10 for SD, whereas the gradual decrease in IC was obtained for GD (Fig. 4) by controlling the initial volume of 0.01 M solution in concentration controller (Fig. 5). Note that deionized water

(electrical resistivity > 180 MΩ·mm, dissolved oxygen concentration < 10 ppb) was used in all column experiments.

A peristaltic pump was used to achieve a constant flow rate, and a pulse dampener was installed between the peristaltic pump and the soil column to reduce the pulsation effect induced by the peristaltic pump. The relatively high-volume pulse dampener was also used as a concentration controller for GD (Fig. 5), whereas the low-volume (~ 50 mL) pulse dampener was installed for SD to obtain a sudden decrease in IC without significant delay. Note that the required volume of 0.01 M NaCl solution to be filled in the pulse dampener to reach an IC = 0 M at PV = 15 was 534 mL for K3 sand and 554 mL for K5 sand (K6 sand was not used in the GD case), calculated by solving the ordinary differential equation (see details in Choe et al. (2022)). A three-way valve was used to decrease the IC to 0.001 and 0 M at PV = 5 and 10 (Fig. 5). A good agreement between analytical and measured IC was obtained for GD and SD, as shown in Fig. 4.

The perforated aluminum disks were placed at the inlet and outlet of the column to obtain a uniform distribution of the injected solution throughout the entire cross-sectional area of the soil column. Plastic meshes (opening size = 74 μm) were placed between the disk and the sample at the outlet to prevent the loss of sand particles during the injection. A schematic of the experimental setup for upward flow is shown in Fig. 5.

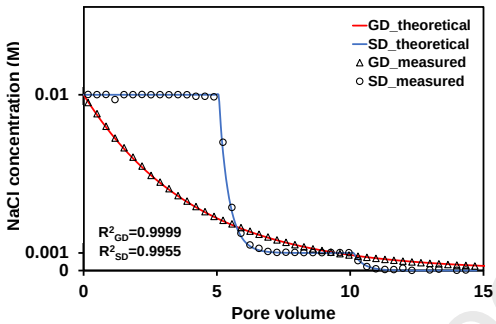

Fig. 4. Theoretical and measured inlet NaCl concentrations for the gradual decrease (GD) and stepwise decrease (SD) in this study.

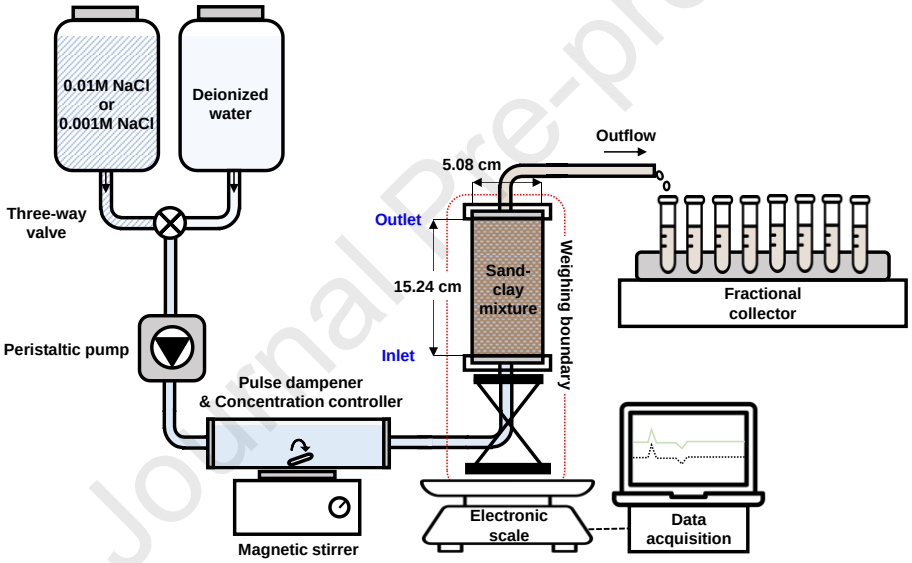

Fig. 5. Schematic drawing of the experimental setup (upward flow). Note that the inlet and outlet of the soil column are flipped for downward flow.

Eluded samples were obtained every 30 mL by placing a fractional collector at the column outlet to determine the concentration of eluded clay (C). A turbidimeter with a measuring range of 0–1000 NTU and an accuracy of ±0.5% was employed to determine the eluded clay concentration of the collected samples using predetermined calibrations (Fig. 6). From the observed BTCs, the mass fraction of the eluded clay (M_e) was determined by calculating the area below the BTC using the trapezoidal method. To quantitatively compare the M_e values between upward and downward flow conditions, R value was defined as follows:

$$R = M_{e\,(up)}/M_{e\,(down)} \quad (2)$$

where $M_{e\,(up)}$ and $M_{e\,(down)}$ represent the M_e values for upward and downward flow experiments, respectively.

For unsaturated conditions, an electronic scale with an accuracy of 0.01 g was placed beneath the soil column to measure the weight of water filled in the column during the injection. To assess the amount of water in sand-clay mixtures relative to the pore volume of the sand matrix, the relative saturation rate (S_r) was defined as follows:

$$S_r = \frac{V_w}{V_p} \times 100\% \quad (3)$$

where the volume of water in the sand-clay mixture (V_w) is derived from the weight of water, and the pore volume of the sand matrix corresponding to the relative density of 70% (V_p) was 128.86, 134.16, and 134.18 mL for K3, K5, and K6 sands, respectively. As shown in Fig. 7, the S_r reached the convergence state, defined as maintaining the S_r within ±1% variation over a range of more than 1 pore volume from a specific point, after injecting a solution of several PVs. From the evolution of the S_r, the average value of the convergence state ($S_{r,Conv}$) and the PV at which saturation convergence begins (PV_{Conv}) were determined (Fig. 7). In addition, M_e values at 3–15 PVs ($M_{e\,(3\text{-}15\ PVs)}$) were also calculated for unsaturated conditions to assess suffusion after saturation convergence.

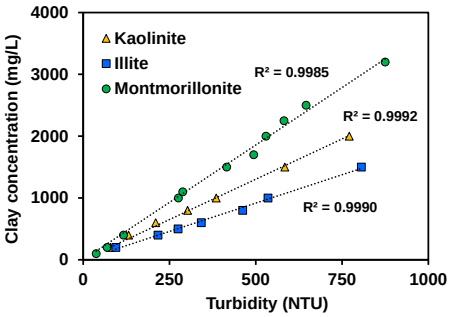

Fig. 6. Calibration results of turbidity vs. clay concentration of suspension.

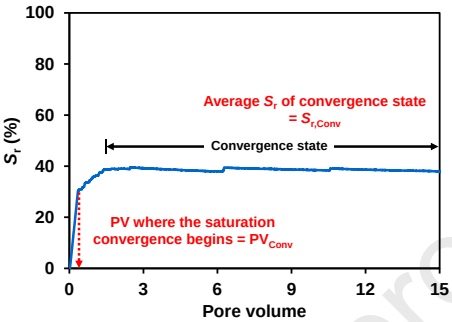

Fig. 7. Determination of $S_{r,Conv}$ and PV_{Conv} from the obtained relative saturation rate (S_r) profile (K3-illite mixtures for SD under downward flow condition).

2.3. Reattachment column test

In this study, additional column tests, referred to as reattachment column tests, were performed using an acrylic column with a greater height of 30.48 cm to confirm the reattachment effect of kaolinite and illite. These experiments were conducted under downward flow conditions at SD, employing soil mixtures of K6 sand mixed with kaolinite or illite. To obtain retention profiles along the soil column, the mass of clay retained in the soil column was calculated by taking samples every 2.54 cm along the column (resulting in 12 samples) and measuring the turbidity of the suspension for each sampled soil (for detailed procedures, refer to Won et al. (2023)).

2.4. Batch detachment test

The batch detachment test was performed to assess the detachment behavior of kaolinite and illite caused by the decrease in IC. 10 g of K6 sand was mixed with clay suspension (clay concentration = 500 mg/L) in 15 mL conical tubes before placing them in the rotation shaker. 0.01 or 0.001 M NaCl solution was initially used as a background solution to induce the sufficient attachment of clay particles during the rotation for 2 h. Then, ~ 8 mL of supernatant in the tube was replaced with deionized water to induce the detachment. From the measured clay concentration in the supernatant, the detachment of clay was assessed at the elapsed time of 5, 10, 20, 30, 60, and 120 min after replacing the solution with deionized water. Because only two-thirds of the solution was replaced with deionized water (solution within the sand and clay cannot be replaced), the final IC was 0.0033 and 3.3×10^{-4} M for an initial IC of 0.01 and 0.001 M, respectively.

2.5. Experimental conditions

A total of 36 cases of soil column experiments were performed, with 18 cases under upward flow conditions and 18 cases under downward flow conditions. For each flow direction, there were 9 cases of GD and 9 cases of SD setups. Three types of sand, three types of clay, two saturated conditions (saturated and unsaturated), and two IC gradients (GD and SD) were selected to investigate the influence of the flow direction, clay type, sand type, and IC gradient on the suffusion in sand-clay mixtures at a given flow rate of 15 mL/min. All experimental conditions conducted in this study are summarized in Table 3. It should be noted that under saturated conditions, the sand-montmorillonite mixture with a clay content of 2.6% was placed in the column to maintain a relative density of the sand matrix at 70%, accounting for the swelling characteristics of montmorillonite.

Table 3
Experimental conditions.

Variable	Saturated condition	Clay type	Sand type	Clay content (%)	Flow direction	Injection method
Flow direction (Section 3.1)	Saturated	Kaolinite	K3	3	Up	GD
					Down	
		Illite			Up	
					Down	
		Montmorillonite		2.6	Up	
					Down	
Clay type (Section 3.2)	Unsaturated	Kaolinite	K3, K5	3	Up	GD
						SD
					Down	GD
						SD
		Illite			Up	GD
						SD
					Down	GD
						SD
		Montmorillonite			Up	GD
						SD
					Down	GD
						SD
Sand type	Unsaturated	Kaolinite	K3*, K5*,	3	Up	SD

(Section 3.3)			K6		Down	
		Illite			Up	
					Down	
		Montmorillonite			Up	
					Down	

*Overlapped cases with experiments in the clay type (Section 3.2).

3. Results and discussion

3.1. Impact of flow direction under saturated conditions

Fig. 8 illustrates the obtained BTCs for saturated K3 sand-clay mixtures under upward and downward flow conditions for GD. For kaolinite and illite (Fig. 8a and b), higher eluded clay concentrations were observed in the downward flow compared to the upward flow. This phenomenon can be attributed to the gravitational effect, given the large specific gravity of kaolinite and illite (G_s = 2.47 and 2.71 for kaolinite and illite, respectively, as shown in Table 2). The direction of downward flow aligns with the settling direction of detached clay particles, resulting in substantial net forces acting on these particles. In contrast, during upward flow, the direction of hydrodynamic forces opposes gravity, leading to lower clay particle velocity within the sand matrix. This observation is consistent with previous studies that found more significant suffusion of saturated gap-graded coarse-grained soils during downward flow (Zhou et al., 2020; Ma et al., 2021; Xiong et al., 2021; Liu et al., 2023). Therefore, a qualitatively consistent impact of flow direction on suffusion is expected for non-swelling clay compared to that observed for small coarse-grained soils.

However, an opposite trend in the concentration of eluded clay between upward and downward flows was observed in the saturated K3-montmorillonite mixtures (Fig. 8c). This phenomenon can be attributed to the high swelling and aggregation potential of montmorillonite particles, which likely results in the significant development of preferential flow paths within the sand-montmorillonite mixtures under a constant flow rate. The swollen montmorillonite particles, or clusters in an aggregated state, may encounter difficulty passing through relatively narrow pore throats, leading to the reattachment or clogging of montmorillonite particles. Consequently, this process reduces the hydraulic conductivity of the mixture by impeding pore water flow under a constant flow rate, thereby resulting in the development of preferential flow paths to alleviate the increased pore water pressure. This suggests that the transported montmorillonite is likely to move through preferential flow paths that formed during the injection process. Because upward flow goes against gravity, the reattachment (or clogging of the relatively smaller pores) by detached montmorillonite particles becomes more significant in upward flow, owing to the lower particle transport velocity. Therefore, more significant preferential flow channels, characterized by fewer flow channels with larger radii, tend to form when the flow is upward as opposed to downward. During upward flow, distinct preferential flow channels were observed in the acrylic column, as visually indicated in Fig. 9. The high eluded montmorillonite concentration at PV < 3 for upward flow (Fig. 8c) suggests that hydraulic-induced suffusion of montmorillonite particles dominates at the given flow rate, because interaction energy-induced suffusion is less likely to occur due to relatively high IC at PV < 3. This observation further supports the substantial formation of preferential flow channels, which leads to high hydrodynamic forces acting on montmorillonite particles under a constant flow rate. Overall, the reverse trend in observed BTCs between non-swelling clays (kaolinite and illite) and swelling clay (montmorillonite) underscores the importance of considering the swelling potential in flow direction-dependent suffusion of sand-clay mixtures.

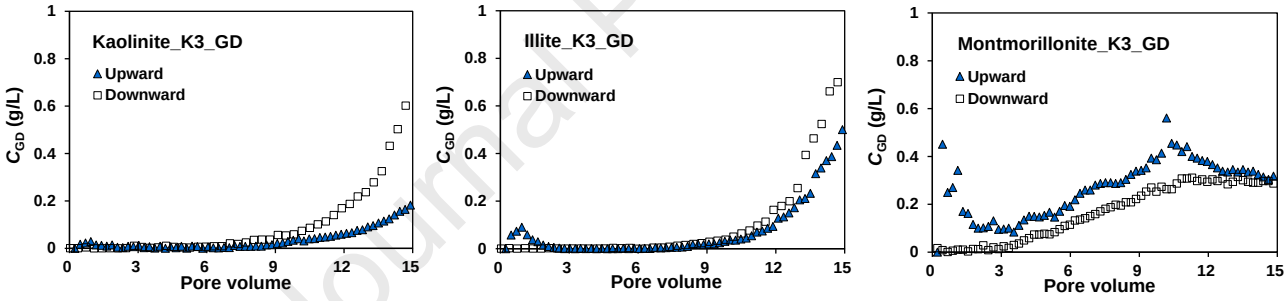

(a) (b) (c)

Fig. 8. Observed BTCs of K3 sand-clay mixtures for (a) kaolinite, (b) illite, and (c) montmorillonite under upward and downward flow conditions at GD experiments.

Fig. 9. Preferential flow channels formed in the K3-montmorillonite mixture column under upward flow conditions.

Table 4 presents the M_e values and the ratio of M_e values between upward and downward flows (R) for the observed BTCs in Fig. 8. Although less significant suffusion under downward flow compared to upward flow was observed for the sand-montmorillonite mixtures (R = 1.28), the higher M_e values of 2.77% for montmorillonite, in contrast to those for kaolinite (M_e = 1.48%) and illite (M_e = 1.64%) suggests the susceptibility of suffusion for swelling clay, regardless of flow direction, at Darcy's velocity of 0.74 cm/min.

Table 4

M_e (mass fraction of eluded clay) and R values of the observed BTCs presented in Fig. 8.

Clay	Sand	Method	Flow direction	$M_{e\ (0\text{-}15\ PVs)}$ (%)	$R_{(0\text{-}15\ PVs)}$
Kaolinite	K3	GD	Up	0.46	0.31
			Down	1.48	
Illite			Up	0.93	0.57
			Down	1.64	
Montmorillonite			Up	3.56	1.28
			Down	2.77	

3.2. Impact of clay type under unsaturated conditions

The BTCs and the relative saturation rate (S_r) of unsaturated K3 and K5 sand-clay mixtures under upward and downward flow conditions for GD and SD are shown in Figs. 10–12. Notably, a higher eluded clay concentration was observed under upward flow compared to downward flow for the sand-kaolinite (Fig. 10) and sand-illite mixtures (Fig. 11), which is the reverse trend compared to saturated conditions (Fig. 8). This shift can be attributed to the lower S_r observed for downward flow as shown in Figs. 10 and 11. A higher S_r leads to a greater fraction of clay particles experiencing detachment because detachment can occur in a sand-water-clay system due to double-layer repulsion. The relatively low S_r for downward flow implies a significant portion of the pore volume in sand-clay mixtures remained dry during injection, suggesting that clay particles are less subjected to the detachment under downward flow than under upward flow. Because suffusion of clay particles is initiated by detachment (with some detached clay particles potentially undergoing reattachment), the more significant suffusion under upward flow than under downward flow indicates that flow direction can be a critical factor in suffusion of sand-clay mixtures under unsaturated as well as saturated conditions. It can be noted that the increased double-layer repulsion typically prevails over interparticle attractions such as van der Waals and capillary attraction when the degree of saturation exceeds about 80% (Lu and Likos, 2006; Likos et al., 2019), which is a consistent tendency with the $S_{r,Conv} > 80\%$ for the sand-kaolinite and sand-illite mixtures, as listed in Table 5.

Additionally, a lower eluded kaolinite concentration was observed under upward flow compared to downward flow for the K5-kaolinite mixture in the SD scenario (Fig. 10d), which differs from the trends observed in other experimental conditions in Figs. 10 and 11. This discrepancy can be attributed to the more significant detachment expected for upward flow, due to that the higher S_r for upward flow as mentioned earlier was compensated by a less pronounced reattachment effect for downward flow compared to upward flow. The higher hydrodynamic forces attributed to the lower S_r for downward flow might result in less reattachment of detached kaolinite particles under downward flow conditions. The higher hydrodynamic forces for downward flow are also expected for the K3-kaolinite mixture (Fig. 10b). However, the higher eluded kaolinite concentration for upward flow indicates a less significant reattachment effect for the K3-kaolinite than the K5-kaolinite mixture. This is likely due to the relatively larger pore sizes of K3 sand compared to K5 sand, reducing the chances of reattachment of detached kaolinite particles in K3 sand. Consequently, the more substantial detachment resulted in a more substantial suffusion for upward flow compared to downward flow for the K3-kaolinite mixture in the SD scenario. Furthermore, the opposite trends between upward and downward flow conditions in GD and SD scenarios of K5-kaolinite mixtures (Fig. 10c and d) indicate the importance of considering the IC gradient. The lower kaolinite concentration observed under downward flow compared to upward flow conditions for GD (Fig. 10c) can be attributed to the more pronounced reattachment effect resulting from the relatively higher likelihood of forming preferential flow paths under downward flow conditions. This observation is supported by the lower S_r under downward flow compared to upward flow conditions and the sudden increase in kaolinite concentration only under downward flow conditions (e.g. a sudden increase in C_{GD} at PV $\approx$ 13.5). In contrast, the higher C_{SD} under downward flow compared to upward flow conditions (Fig. 10d), particularly after the sudden decrease in IC from 0.001 to 0 M, suggests that a high IC gradient led to a reduced reattachment effect under downward flow conditions. The higher fraction of detached kaolinite particles resulted in more suffusion under downward flow compared to upward flow conditions, as evidenced by the lower S_r observed during downward flow.

Meanwhile, the higher eluded clay concentration observed for the K5-illite mixture (Fig. 11d) compared to the K5-kaolinite mixture (Fig. 10d) under upward flow conditions suggests a less significant reattachment effect for detached illite particles compared to kaolinite particles or more significant detachment of illite driven by the sudden decrease in IC from 0.001 to 0 M. This difference can be attributed to the fact that the interaction energy between sand and clay is also influenced by clay mineralogy (Bradford and Blanchar, 1999; Won et al., 2021; Choe et al., 2022).

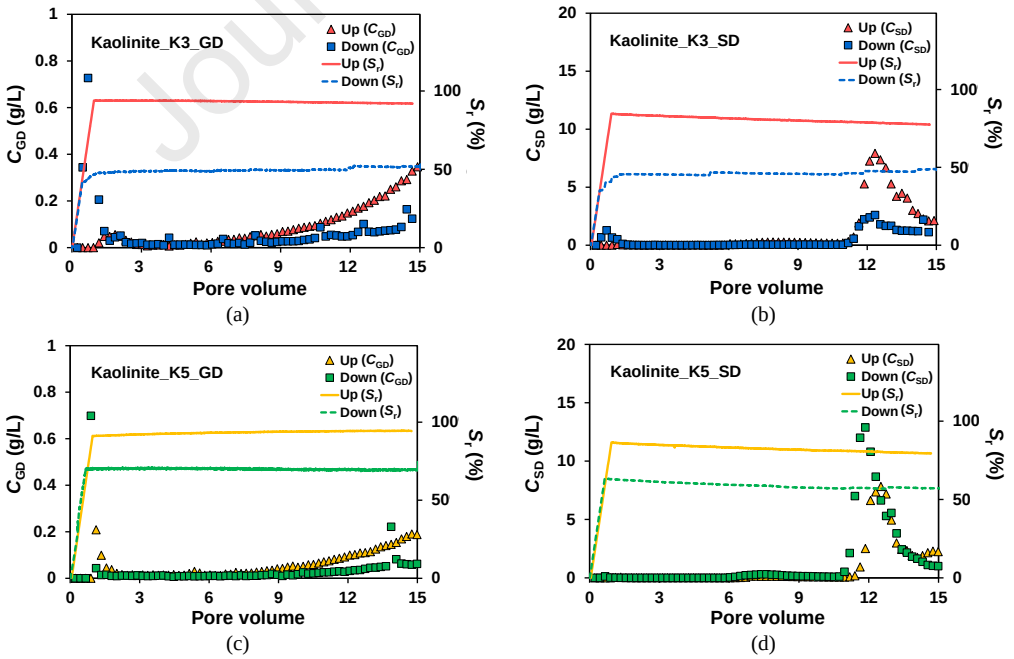

Fig. 10. Observed BTCs and relative saturation rate (S_r) profiles of sand-kaolinite mixtures under upward and downward flow conditions for K3 sand (a, b) and K5 sand (c, d) at GD (a, c) and SD (b, d) experiments.

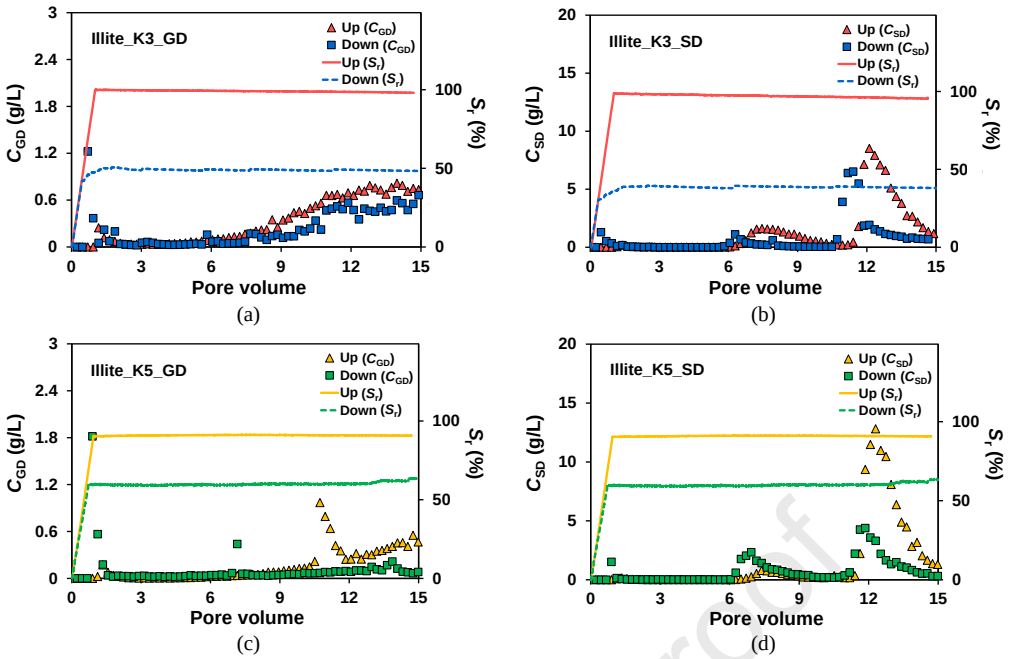

Fig. 11. Observed BTCs and relative saturation rate (S_r) profiles of sand-illite mixtures under upward and downward flow conditions for K3 sand (a, b) and K5 sand (c, d) at GD (a, c) and SD (b, d) experiments.

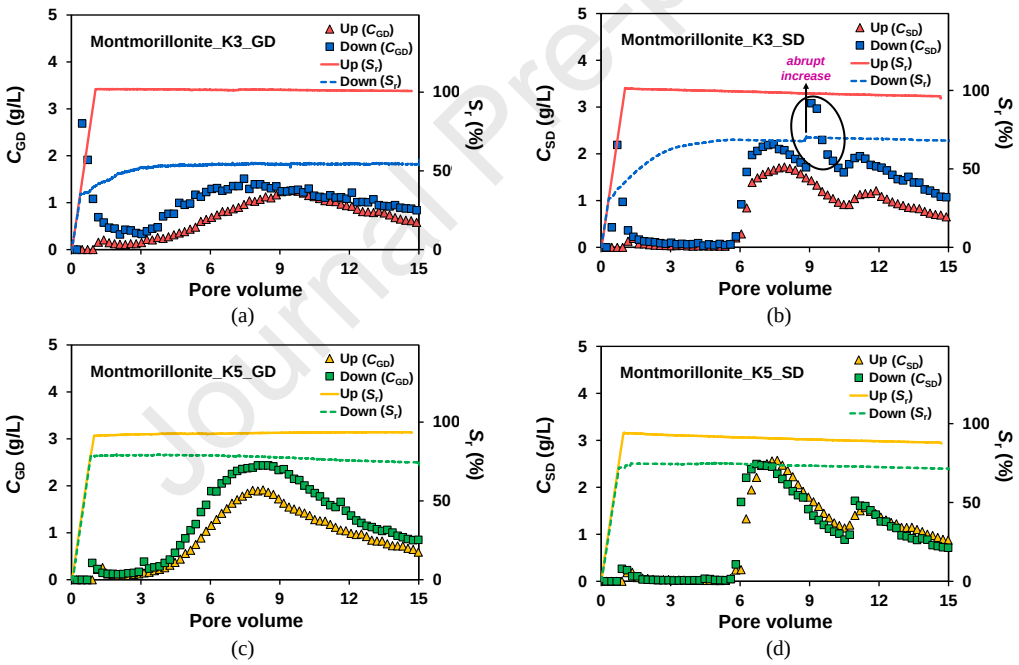

Fig. 12. Observed BTCs and relative saturation rate (S_r) profiles of sand-montmorillonite mixtures under upward and downward flow conditions for K3 sand (a, b) and K5 sand (c, d) at GD (a, c) and SD (b, d) experiments.

It should be noted that a higher eluded clay concentration at low PVs (< 3) was observed under downward flow compared to upward flow for all clay types (Figs. 10–12). In upward flow, the soil column is expected to saturate relatively uniformly with a gradual rise in the water level, whereas the initial formation of relatively preferential flow paths is expected during saturation for downward flow (Fig. 13). This can be inferred from the higher $S_{r,Conv}$ and PV_{Conv} values (Table 5) for upward flow compared to downward flow. Therefore, more hydraulic-induced suffusion could occur at low PVs (< 3) under downward flow than under upward flow due to the high hydrodynamic forces caused by the initial formation of preferential flow paths, even at relatively high NaCl concentrations with high attraction energy between clay and sand (i.e. IC = 0.005 M for GD and 0.01 M for SD at PV = 3). The difference between $M_{e\,(3\text{-}15\ PVs)}$ and $M_{e\,(0\text{-}15\ PVs)}$, as shown in Table 6, quantitatively represents hydraulic-induced suffusion at PV < 3. Similar values of $M_{e\,(3\text{-}15\ PVs)}$ and $M_{e\,(0\text{-}15\ PVs)}$ indicate almost no hydraulic-induced suffusion occurred under upward flow.

In contrast to the sand-kaolinite and sand-illite mixtures, the sand-montmorillonite mixtures mostly exhibited a higher concentration of eluded montmorillonite under downward flow than under upward flow (Fig. 12). This suggests that the initial formation of preferential flow paths under downward flow (characterized by lower S_r for downward flow) more significantly induces the suffusion of montmorillonite particles than upward flow. Therefore, it can be concluded that detachment has a more critical impact on suffusion for kaolinite and illite, whereas the formation of preferential flow paths is more critical than the detachment potential (or S_r) when assessing the susceptibility of suffusion for the sand-montmorillonite mixtures under unsaturated conditions. The dominance of preferential flow becomes less significant for SD under a relatively low SR, which is supported by the similar eluded montmorillonite concentrations for the K5-montmorillonite mixtures in the SD scenario (R = 1.02 (Table 6)). The relatively similar R values between K3-montmorillonite (R = 0.65) and K5-montmorillonite mixtures (R = 0.71) for GD, compared to those for SD (R = 0.6 and 1.02 for the K3-montmorillonite and K5-montmorillonite mixtures, respectively), suggest that the dominance of the preferential flow effect over the detachment effect

for suffusion of swelling clay can be influenced by the IC gradient under unsaturated conditions. For the K5-montmorillonite mixtures under SD, R = 1.02 indicates that the montmorillonite particles abruptly detached by suffusion were not significantly affected by gravitational forces under high hydrodynamic forces. Therefore, it can be inferred that the combined effect of abrupt detachment and high hydrodynamic forces can lead to suffusion independent of flow direction for swelling clay. In contrast, R < 1 for the remaining three cases suggests that the gravitational effect becomes significant under conditions of gradual detachment or low hydrodynamic forces for swelling clay.

In summary, a reverse trend of the eluded clay concentration as a function of flow direction was observed for kaolinite, illite, and montmorillonite between saturated and unsaturated conditions. For the sand-kaolinite and sand-illite mixtures, R < 1 under saturated conditions (Table 4) and R > 1 under unsaturated conditions (Table 6). Conversely, for the sand-montmorillonite mixtures, R > 1 under saturated conditions (Table 4) and R < 1 under unsaturated conditions (Table 6). Therefore, it can be concluded that the impact of flow direction on the suffusion of sand-clay mixtures is strongly dependent on the saturation state.

It can be noted that S_r profiles for several experimental cases showed an abrupt increase during the injection, corresponding to the convergence state as seen in Fig. 7. This phenomenon can be attributed to the rearrangement of pore structures due to the formation of additional flow paths during the injection (Choe et al., 2022). This observation is particularly pronounced for the K3-clay mixtures under downward flow conditions, irrespective of clay types, as shown in Figs. 10a, b, 11a, b, and 12a, b. For example, the abrupt increase in montmorillonite concentration and S_r observed at PV ≈ 9 under downward flow conditions for SD (Fig. 12b) demonstrates that the sudden loss of montmorillonite particles led to the formation of additional flow paths. In addition, similar observations of the sudden increase in kaolinite (e.g. PV ≈ 13.5 in Fig. 10c) and illite concentration (e.g. PV ≈ 7 and 10 in Fig. 11c) can also be attributed to the formation of additional flow paths induced by the sudden filtration of reattached clay particles near the outlet.

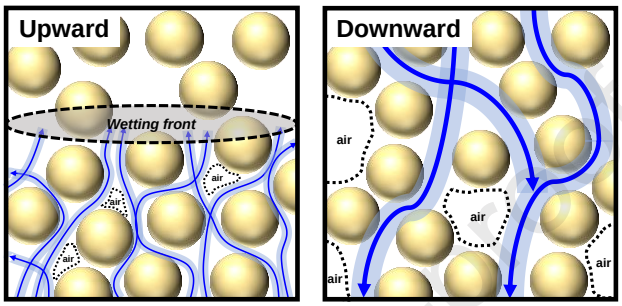

(a) (b)

Fig. 13. Schematic drawings of the water flow in sand-clay mixtures under (a) upward and (b) downward flow conditions (clay particles were ignored).

Table 5

PV_{Conv} and $S_{r,Conv}$ values for experiments in Figs. 10–12.

Clay	Sand	Method	Flow direction	PV_{Conv} (PVs)	$S_{r,Conv}$ (%)
Kaolinite	K3	GD	Up	0.94	93
			Down	0.45	50
		SD	Up	0.89	81
			Down	0.39	46
	K5	GD	Up	0.96	93
			Down	0.67	70
		SD	Up	0.92	83
			Down	0.64	59
Illite	K3	GD	Up	1.01	99
			Down	0.44	49
		SD	Up	1.02	97
			Down	0.34	39
	K5	GD	Up	0.93	91
			Down	0.71	60
		SD	Up	0.95	87
			Down	0.71	59
Montmorillonite	K3	GD	Up	1.03	101
			Down	0.37	54
		SD	Up	1.04	99
			Down	0.33	68
	K5	GD	Up	0.97	93
			Down	0.83	78
		SD	Up	0.95	91
			Down	0.76	74

Note: PV_{Conv} = injected pore volume initiating the saturation convergence; $S_{r,Conv}$ = average S_r after saturation convergence until the end of the experiment.

Table 6

M_e (mass fraction of eluded clay) and R values of the observed BTCs presented in Figs. 10–12.

Clay	Sand	Method	Flow direction	$M_{e\ (3\text{-}15\ PVs)}$ (%)	$R_{(3\text{-}15\ PVs)}$	$M_{e\ (0\text{-}15\ PVs)}$ (%)	$R_{(0\text{-}15\ PVs)}$
Kaolinite	K3	GD	Up	1.05	2.32	1.11	1.09
			Down	0.45		1.02	
		SD	Up	14.96	2.87	15	2.53
			Down	5.21		5.92	
	K5	GD	Up	0.7	2.18	0.8	1.6
			Down	0.32		0.5	
		SD	Up	12.7	0.64	12.74	0.65
			Down	19.7		19.74	
Illite	K3	GD	Up	4.01	1.57	4.15	1.37

			Down	2.56		3.03	
		SD	Up	17.24	1.95	17.34	1.85
			Down	8.83		9.38	
	K5	GD	Up	2.2	2.47	2.28	1.53
			Down	0.89		1.49	
		SD	Up	21.84	2.12	21.94	2.05
			Down	10.31		10.72	
Montmorillonite	K3	GD	Up	8.56	0.74	8.78	0.65
			Down	11.62		13.55	
		SD	Up	9.34	0.63	9.47	0.6
			Down	14.8		15.82	
	K5	GD	Up	12.41	0.71	12.67	0.71
			Down	17.42		17.77	
		SD	Up	13.48	1.02	13.63	1.02
			Down	13.17		13.36	

The calculated M_e values for every 5 PVs concerning the BTCs in Figs. 10–12 are compared in Fig. 14. In the case of sand-kaolinite and sand-illite mixtures (Fig. 14a and b), the total M_e values for SD were higher than those for GD, with the highest $M_{e\ (10\text{-}15\ PVs)}$ observed for both SD and GD. This indicates that the suffusion of kaolinite and illite particles is particularly susceptible to the sudden decrease in IC, especially a decrease from 0.001 to 0 M. In contrast, only slightly higher total M_e values were observed under SD compared to GD for the sand-montmorillonite mixtures at the given flow direction and sand type, except for the K5-montmorillonite mixtures under downward flow (Fig. 14c). Therefore, the impact of IC gradient more critically affects the suffusion of non-swelling clay compared to swelling clay under unsaturated conditions. Note that the more significant suffusion of the unsaturated sand-kaolinite and sand-illite mixtures under SD than GD for downward flow aligns with the trends observed under saturated conditions for identical experimental conditions (Choe et al., 2022).

Among three M_e values, the highest $M_{e\ (5\text{-}10\ PVs)}$ was observed for the sand-montmorillonite mixtures (Fig. 14c), even though the IC was higher at 5–10 PVs compared to 10–15 PVs. This can be attributed to the swelling kinetics of montmorillonite particles (Chen et al., 2016; Proia et al., 2016; Magzoub et al., 2017, 2020). Because initially dry montmorillonite particles require a certain amount of time to reach a fully-swelling state, it is expected that montmorillonite particles are relatively smaller in size at PV = 5–10 compared to highly-swollen montmorillonite particles at PV = 10–15. Magzoub et al. (2020) reported that approximately 3 h is required for montmorillonite to achieve full hydration. This suggests that montmorillonite particles during the injection in this study were in the process of swelling (15 PVs correspond to the injection time of 128.86 and 134.16 min for the K3-montmorillonite and K5-montmorillonite mixtures, respectively). Therefore, the intermediately low IC and swollen montmorillonite contributed to the most substantial suffusion at PV = 5–10.

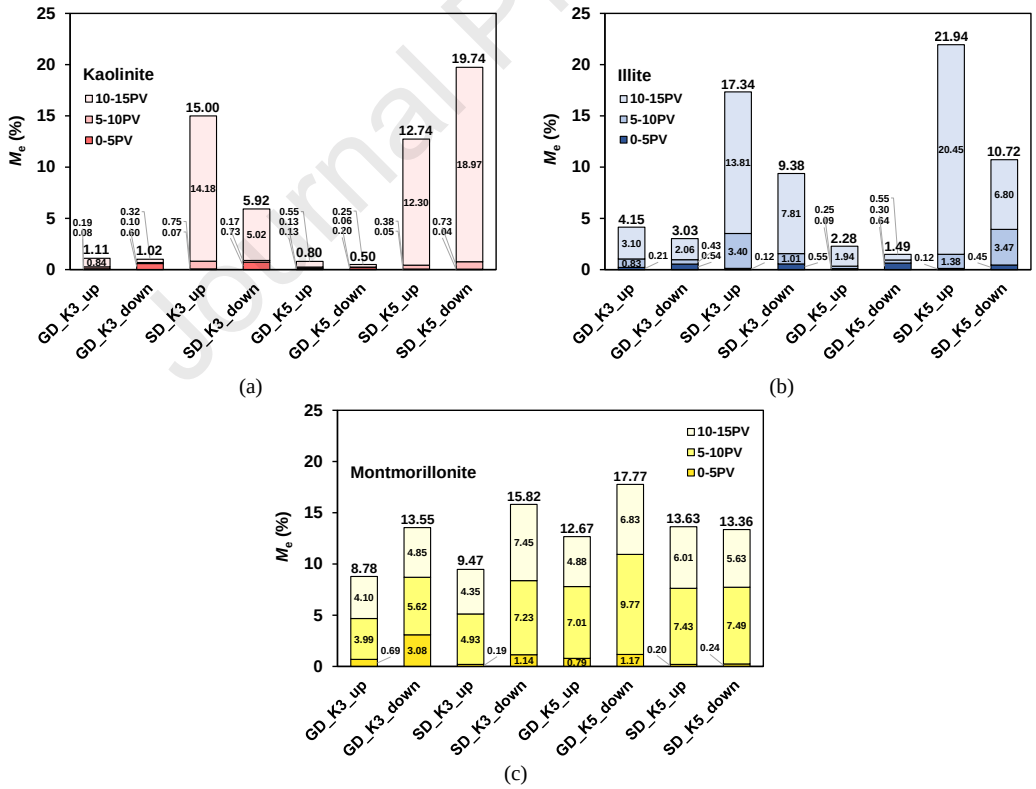

Fig. 14. M_e values for 15 PVs (numbers at the top of bars), 0–5 PVs, 5–10 PVs, and 10–15 PVs for the BTCs presented in Figs. 10–12.

3.3. Impact of sand type under unsaturated conditions

Fig. 15 illustrates the BTCs and the relative saturation rate (S_r) of unsaturated sand-clay mixtures under upward flow conditions (Fig. 15a, c, and e) and under downward flow conditions (Figs. 15b, d, and f) for the SD scenario. The highest eluded kaolinite concentration was observed for the K6-kaolinite mixtures (SR = 45) as shown in Fig. 15a and b, whereas the lowest eluded illite concentration was observed for the K6-illite mixtures (SR = 52) as shown in Fig. 15c and d. Since the suffusion of sand-clay mixtures is dependent on detachment and reattachment effects (Choe et al., 2022; Won, 2022; Won et al., 2023), reattachment column tests with a 30.48 cm column and batch detachment tests were performed for the K6-kaolinite and K6-illite mixtures for the SD scenario as shown in Figs. 16 and 17, respectively. As described in Fig. 16a, even less total illite than kaolinite was observed at the outlet, which is consistent with the BTCs in Fig. 15b and d for the 15.24 cm column. The slightly higher retained illite content than kaolinite content with depth (Fig. 16b) after injection indicates less substantial detachment or more significant reattachment of illite than kaolinite particles. The batch

detachment tests revealed that greater detachment of illite (38.5 mg/L) than kaolinite (17.38 mg/L) occurred when IC was reduced from 0.01 to 0.0033 M, whereas more significant detachment of kaolinite (75.05 mg/L) than illite (32.65 mg/L) occurred when IC was reduced from 0.001 to 0.00033 M (Fig. 17 and Table 7). Therefore, the higher eluded kaolinite concentration than illite at PV = 5–10 (IC reduced from 0.01 to 0.001 M) indicates the more significant reattachment of illite than kaolinite particles in the 30.48 cm column. The even higher eluded kaolinite concentration than illite at PV = 10–15 (Fig. 16a) can be attributed to the combined effect of less detachment and more significant reattachment of illite than kaolinite particles. Because the reattachment effect is a function of pore sizes, the reattachment effect for the K3-illite and K5-illite mixtures becomes less significant, as shown in Fig. 15c and d.

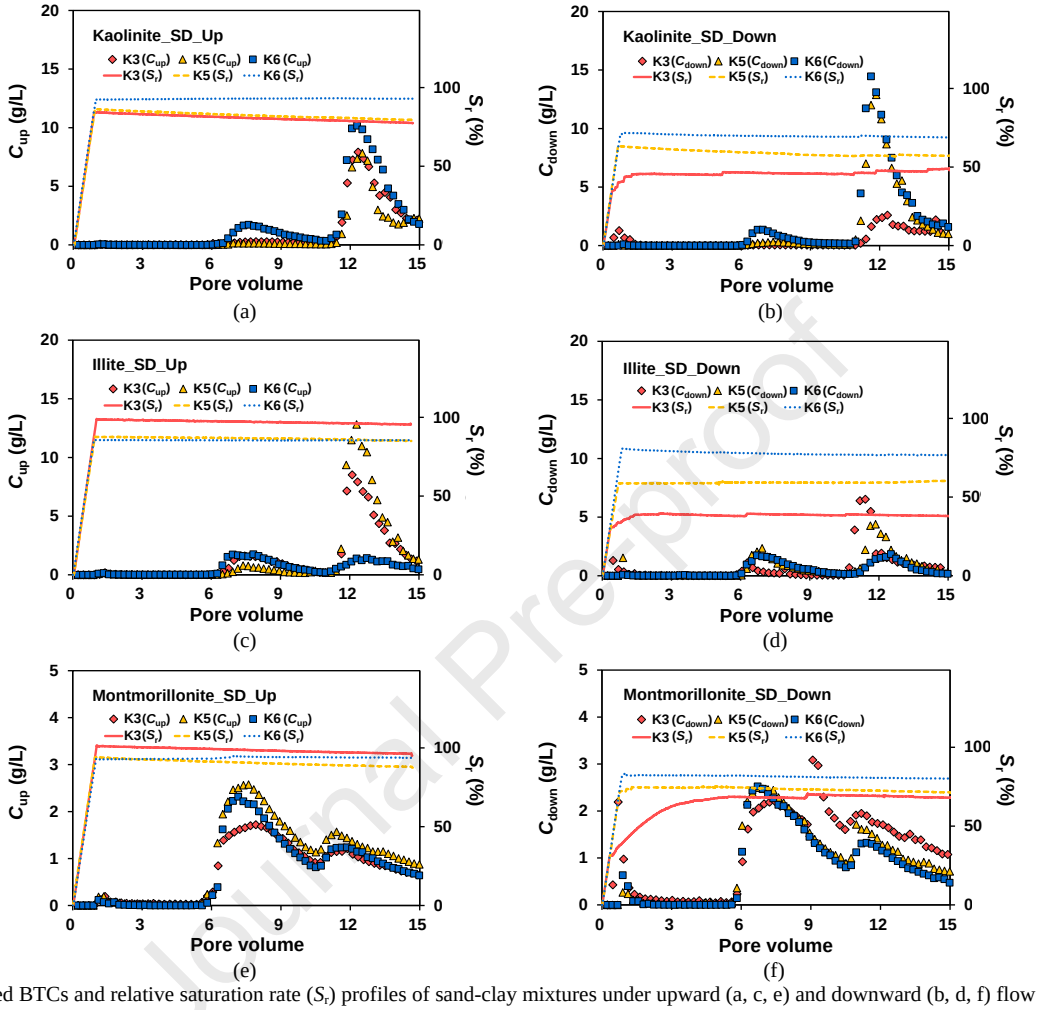

Fig. 15. Observed BTCs and relative saturation rate (S_r) profiles of sand-clay mixtures under upward (a, c, e) and downward (b, d, f) flow conditions for kaolinite (a, b), illite (c, d), and montmorillonite (e, f) in SD scenario.

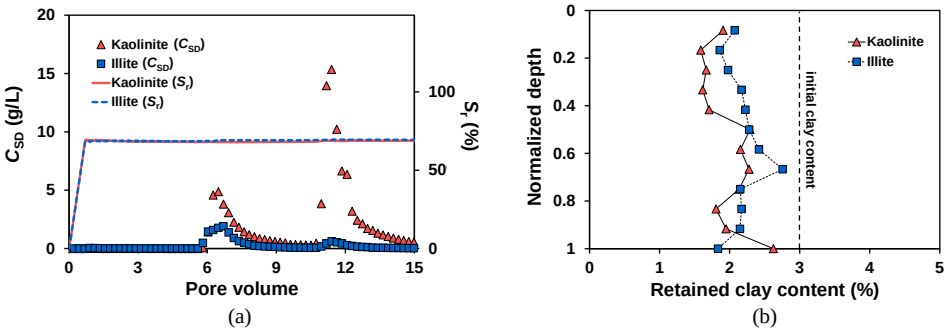

Fig. 16. Obtained (a) BTCs and relative saturation rate (S_r) profiles, and (b) retention profiles of K6-kaolinite and K6-illite mixtures under downward flow conditions at SD in reattachment column tests.

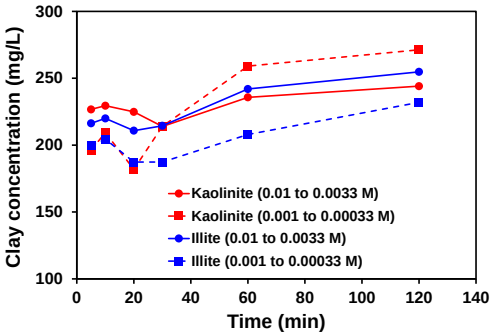

Fig. 17. The detached kaolinite and illite concentration at the elapsed time from 5 to 120 min in batch detachment tests.

Table 7
Detached clay concentration of kaolinite and illite obtained from Fig. 17. All clay concentrations are in mg/L.

Experimental condition	Clay concentration (t = 5 min)	Clay concentration (t = 120 min)	Detached clay concentration
Kaolinite (0.01 to 0.0033 M)	226.7	244.08	17.38
Kaolinite (0.001 to 0.00033 M)	196.23	271.28	75.05
Illite (0.01 to 0.0033 M)	216.31	254.8	38.5
Illite (0.001 to 0.00033 M)	199.35	232	32.65

As seen in Fig. 15e and f, the least substantial suffusion of montmorillonite was observed for the K3-montmorillonite mixture under upward flow (Fig. 15e), whereas the most significant suffusion of montmorillonite was observed for the K3-montmorillonite mixtures under downward flow (Fig. 15f). Similar to the discussion in the previous sections, this can likely be attributed to the lowest hydrodynamic forces for the K3-montmorillonite mixture under upward flow, whereas the highest hydrodynamic forces can be anticipated for the K3-montmorillonite mixture under downward flow, which can be deduced from the lowest $S_{r,Conv}$ (Table 8) and the significant initial concentration of eluded montmorillonite at PV < 3. Under downward flow, the order of $S_{r,Conv}$ (K6 > K5 > K3) is reversely consistent with the order of M_e values (K3 > K5 > K6) as compared in Fig. 18c.

Table 8
PV_{Conv} and $S_{r,Conv}$ values for experiments in Fig. 15.

Clay	Method	Sand (SR)	Flow direction	PV_{Conv} (PVs)	$S_{r,Conv}$ (%)
Kaolinite	SD	K3 (162)	Up	0.89	81
			Down	0.39	46
		K5 (79)	Up	0.92	83
			Down	0.64	59
		K6 (45)	Up	0.97	93
			Down	0.75	70
Illite		K3 (189)	Up	1.02	97
			Down	0.34	39
		K5 (92)	Up	0.95	87
			Down	0.71	59
		K6 (52)	Up	0.91	85
			Down	0.83	78
Montmorillonite		K3 (1700)	Up	1.04	99
			Down	0.33	68
		K5 (830)	Up	0.95	91
			Down	0.76	74
		K6 (470)	Up	0.99	94
			Down	0.86	82

Table 9
M_e (mass fraction of eluded clay) and R values of the observed BTCs presented in Fig. 15.

Clay	Method	Sand (SR)	Flow direction	$M_{e\,(3\text{-}15\ PVs)}$ (%)	$R_{(3\text{-}15\ PVs)}$	$M_{e\,(0\text{-}15\ PVs)}$ (%)	$R_{(0\text{-}15\ PVs)}$
Kaolinite	SD	K3 (162)	Up	14.96	2.87	15	2.53
			Down	5.21		5.92	
		K5 (79)	Up	12.7	0.64	12.74	0.65
			Down	19.7		19.74	
		K6 (45)	Up	24.35	0.98	24.38	0.98
			Down	24.91		24.94	
Illite		K3 (189)	Up	17.24	1.95	17.34	1.85
			Down	8.83		9.38	
		K5 (92)	Up	21.84	2.12	21.94	2.05
			Down	10.31		10.74	
		K6 (52)	Up	8.13	1.16	8.22	1.17
			Down	6.99		7.03	
Montmorillonite		K3 (1700)	Up	9.34	0.63	9.47	0.6
			Down	14.8		15.82	
		K5 (830)	Up	13.48	1.02	13.63	1.02
			Down	13.17		13.36	
		K6	Up	10.84	0.94	10.92	0.93

		(470)	Down	11.52		11.78	

For the sand-kaolinite mixtures, R values showed a significant decrease from R = 2.53 to 0.65 as the sand-grain size decreased from K3 to K5 (Table 9). This indicates the existence of a threshold SR between 162 (for the K3-kaolinite mixture) and 79 (for the K5-kaolinite mixture), where relatively substantial suffusion occurs under downward flow compared to upward flow. In contrast, there was a sharp decrease in R values from R = 1.02 to 0.6 when the sand-grain size increased from K5 to K3 for the sand-montmorillonite mixtures. This can be attributed to the formation of substantial preferential flow paths under downward flow and low hydrodynamic forces applied to montmorillonite particles under upward flow in the K3-montmorillonite mixture.

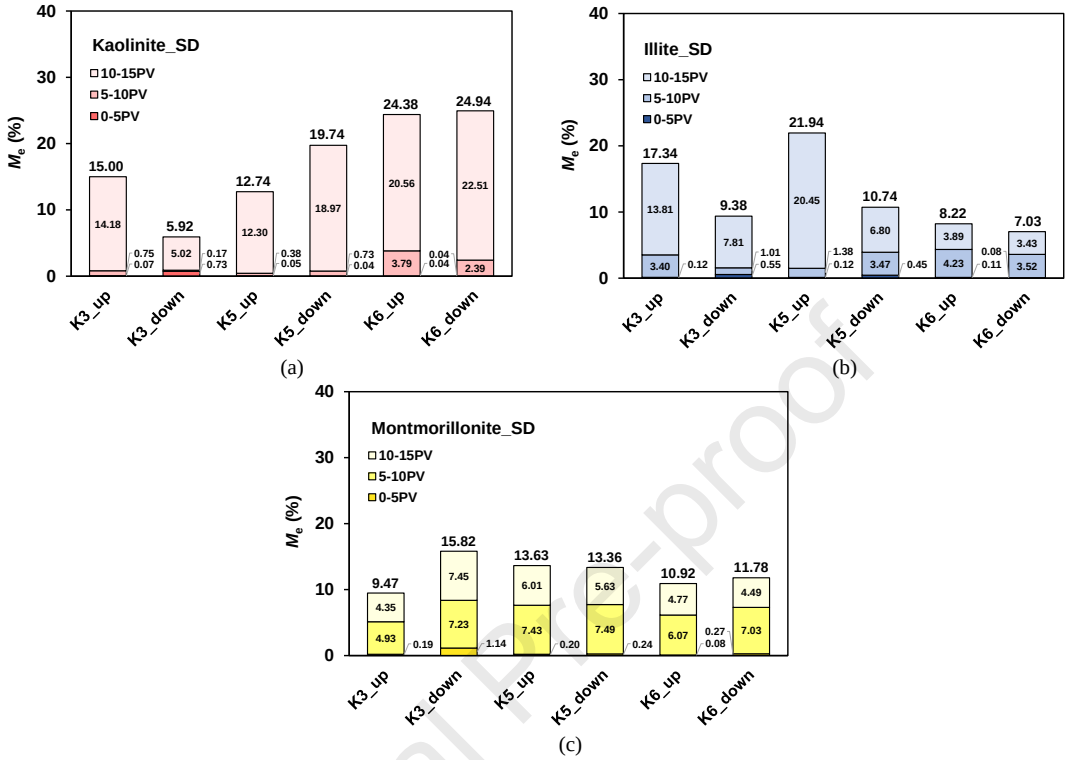

Fig. 18. M_e values for 15 PVs (numbers at the top of bars), 0–5 PVs, 5–10 PVs, and 10–15 PVs for the BTCs presented in Fig. 15.

4. Conclusions

This study conducted soil column experiments to investigate the impact of flow direction on the suffusion of sand-clay mixtures under both saturated and unsaturated conditions. Three types of sand and three types of clay were selected to investigate the influence of the sand-to-clay size ratio and swelling potential on the suffusion of sand-clay mixtures under two scenarios of IC gradients (GD and SD). The following conclusions were drawn based on the observed BTCs, relative saturation rate (S_r), and mass fraction of eluded clay (M_e):

(1) Under saturated conditions, it was observed that more clay particles eluded under downward flow than under upward flow for the K3-kaolinite and K3-illite mixtures, whereas the opposite trend was observed for the K3-montmorillonite mixtures.
(2) Under unsaturated conditions, higher eluded clay concentrations were observed under upward flow compared to downward flow for the K3-kaolinite and K3-illite mixtures regardless of IC gradient (GD and SD). This difference can be attributed to the higher S_r, which leads to more substantial detachment under upward flow conditions.
(3) The higher eluded montmorillonite and lower S_r under downward flow, compared to upward flow, for unsaturated conditions indicate the significant formation of preferential flow paths under downward flow conditions.
(4) The highest $M_{e\ (10\text{-}15\ PVs)}$ values for kaolinite and illite among the three M_e values ($M_{e\ (0\text{-}5\ PVs)}$, $M_{e\ (5\text{-}10\ PVs)}$, and $M_{e\ (10\text{-}15\ PVs)}$) suggest the highest susceptibility to suffusion for kaolinite and illite when IC decreases from 0.001 to 0 M. In contrast, non-fully swollen montmorillonite particles with intermediately low IC led to the highest $M_{e\ (5\text{-}10\ PVs)}$ values for the sand-montmorillonite mixtures.
(5) The trend of R values (= $M_{e\ (up)}$ / $M_{e\ (down)}$) as a function of the size ratio for the sand-kaolinite mixtures suggests the existence of a threshold sand-to-clay size ratio where suffusion induced by downward flow becomes relatively more significant than upward flow under unsaturated conditions.
(6) The findings regarding suffusion tendencies in sand-clay mixtures presented in this study highlight the importance of monitoring crucial factors such as flow direction, saturation state, and swelling potential. This monitoring is essential for assessing the susceptibility to suffusion in clay-containing earthen structures.

Declaration of competing interest

The authors declare that they have no known competing financial interests or personal relationships that could have appeared to influence the work reported in this paper.

Acknowledgments

This study was supported by the Korea Agency for Infrastructure Technology Advancement under the Ministry of Land, Infrastructure and Transport (Grant No. RS-2024-00410248) and by National Research Foundation of Korea (NRF) grants funded by the Korean government (MSIT) (Grant No. RS-2022R1C1C1007296).

References

ASTM D422, 2007. Standard test method for particle-size analysis of soils. American Society of Testing and Materials, West Conshohocken, PA.
ASTM D854, 1999. Standard test method for specific gravity of soils. American Society for Testing and Materials, West Conshohocken, PA, USA.
ASTM D4253, 1996. Test methods for maximum index density and unit weight of soils using a vibratory table. American Society of Testing and Materials, West Conshohocken, PA.
ASTM D 4254, 2006. Standard test methods for maximum index density and unit weight of soils and calculation of relative density. American Society of Testing and Materials, West Conshohocken, PA.
Basha, H. A., Culligan, P. J., 2010. Modeling particle transport in downward and upward flows. Water Resour. Res. 46 (7), 1–17.
Benamar, A., 2014. Effect of hydraulic load and water chemistry on soil suffusion. Proc. Int. Conf. Scour Eros. ICSE, 197–202.
Benamar, A., Correia dos Santos, R. N., Bennabi, A., Karoui, T., 2019. Suffusion evaluation of coarse-graded soils from Rhine dikes. Acta Geotech. 14 (3), 815–823.
Blume, T., Weisbrod, N., Selker, J. S., 2005. On the critical salt concentrations for particle detachment in homogeneous sand and heterogeneous Hanford sediments. Geoderma 124 (1–2), 121–132.
Bradford, J. M., Blanchar, R. W., 1999. Mineralogy and water quality parameters in rill erosion of clay–sand mixtures. Soil Sci. Soc. Am. J. 63 (5), 1300–1307.
Chang, D., Zhang, L., Cheuk, J., 2014. Mechanical consequences of internal soil erosion. HKIE Trans. Hong Kong Inst. Eng. 21 (4), 198–208.
Chen, L., Wan, Y., He, J. J., Luo, C. M., Yan, S. F., He, X. F., 2021. Experimental study on the suffusion mechanism of gap-graded soils under an exceedance hydraulic gradient. Nat. Hazards 109 (1), 405-439.
Chen, Y. G., Zhu, C. M., Ye, W. M., Cui, Y. J., Chen, B., 2016. Effects of solution concentration and vertical stress on the swelling behavior of compacted GMZ01 bentonite. Appl. Clay Sci. 124–125, 11–20.
Chetti, A., Benamar, A., Hazzab, A., 2016. Modeling of particle migration in porous media: Application to soil suffusion. Transp. Porous Media 113 (3), 591–606.
Choe, Y., Choi, H., Won, J., 2022. Suffusion of a sand–clay mixture: impact of the ionic-concentration gradient, clay type, sand-grain size and hydraulic gradient. Géotechnique, 74 (10), 1004-1018.
Chrysikopoulos, C. V., Syngouna, V. I., 2014. Effect of gravity on colloid transport through water-saturated columns packed with glass beads: Modeling and experiments. Environ. Sci. Technol. 48 (12), 6805–6813.
Collins, B. D., Znidarcic, D., 2004. Stability analyses of rainfall induced landslides. J. Geotech. Geoenviron. Eng. 130 (4), 362–372.
Deng, Z., Wang, G., Wang, Z., Jin, W., 2024. Modelling erosion and stability degradation of a reservoir slope under periodic water level fluctuations. Comput. Geotech., 166, 106021.
Fell, R., Fry, J. J., 2007. The state of the art of assessing the likelihood of internal erosion of embankment dams, water retaining structures and their foundations. In: Internal Erosion of Dams and Their Foundations. CRC Press, pp. 1–24.
Fredlund, D. G., Rahardjo, H., Fredlund, M. D., 2012. Unsaturated soil mechanics in engineering practice. Unsaturated Soil Mech. Eng. Pract. 132, 286–321.
Gao, C., 2007. Factors affecting particle retention in porous media. Emirates J. Eng. Res. 12 (3), 1–7.
Hassanizadeh, S. M., Celia, M. A., Dahle, H. K., 1997. Dynamic effect in the capillary pressure–saturation relationship and its impacts on unsaturated flow. Vadose Zone J. 1 (1), 38–57.
Imai, G., 1980. Settling behavior of clay suspension. Soils Found. 20 (2), 61–77.
Israr, J., Indraratna, B., 2019. Study of critical hydraulic gradients for seepage-induced failures in granular soils. J. Geotech. Geoenviron. Eng. 145 (7), 1–15.
Jiang, S., Bai, B., Zhang, P., Le Li, H., Wang, P., 2016. Effect of gravity and particle size distribution on the suspended particle transport and deposition in a saturated porous medium. Fresenius Environ. Bull. 25(12), 5638-5649.
Ke, L., Takahashi, A., 2014. Experimental investigations on suffusion characteristics and its mechanical consequences on saturated cohesionless soil. Soils Found. 54 (4), 713–730.
Kodieh, A., Gelet, R., Marot, D., Fino, A. Z., 2021. A study of suffusion kinetics inspired from experimental data: Comparison of three different approaches. Acta Geotech. 16 (2), 347–365.
Kotlyar, L. S., 1998. Effect of particle size on the flocculation behaviour of ultra-fine clays in salt solutions. Clay Miner. 33 (1), 103–107.
Lei, X., He, S., Chen, X., Wong, H., Wu, L., Liu, E., 2020. A generalized interpolation material point method for modelling coupled seepage-erosion-deformation process within unsaturated soils. Adv. Water Resour. 141, 103578.
Lei, X., Yang, Z., He, S., Liu, E., Wong, H., Li, X., 2017. Numerical investigation of rainfall-induced fines migration and its influences on slope stability. Acta Geotech. 12 (6), 1431–1446.
Liang, Y., Yeh, T. C. J., Zha, Y., Wang, J., Liu, M., Hao, Y., 2017. Onset of suffusion in gap-graded soils under upward seepage. Soils Found. 57 (5), 849–860.
Likos, W. J., Song, X., Xiao, M., Cerato, A., Lu, N., 2019. Fundamental challenges in unsaturated soil mechanics. In: Geotechnical Fundamentals for Addressing New World Challenges. Springer, pp. 209–236.
Liu, Y., Wang, L., Hong, Y., Zhao, J., Yin, Z. Y., 2020. A coupled CFD-DEM investigation of suffusion of gap graded soil: Coupling effect of confining pressure and fines content. Int. J. Numer. Anal. Methods Geomech. 44 (18), 2473–2500.
Liu, Y., Wang, L., Yin, Z. Y., Hong, Y., 2023. A coupled CFD-DEM investigation into suffusion of gap-graded soil considering anisotropic stress conditions and flow directions. Acta Geotech. 18 (6), 3111–3132.
Lu, N., Likos, W. J., 2004. Unsaturated soil mechanics. J. Wiley Hoboken, NJ.
Lu, N., Likos, W. J., 2006. Suction stress characteristic curve for unsaturated soil. J. Geotech. Geoenvironmental Eng. 132 (2), 131–142.
Ma, Q., Wautier, A., Zhou, W., 2021. Microscopic mechanism of particle detachment in granular materials subjected to suffusion in anisotropic stress states. Acta Geotech. 16 (8), 2575–2591.
Magzoub, M. I., Hussein, I. A., Nasser, M. S., Mahmoud, M., Sultan, A. S., Benamor, A., 2020. An investigation of the swelling kinetics of bentonite systems using particle size analysis. J. Dispers. Sci. Technol. 41 (6), 817–827.
Magzoub, M. I. et al., 2017. Effects of sodium carbonate addition, heat and agitation on swelling and rheological behavior of Ca-bentonite colloidal dispersions. Appl. Clay Sci. 147, 176–183.
McDowell-Boyer, L. M., Hunt, J. R., Sitar, N., 1986. Particle transport through porous media. Water Resour. Res. 22 (13), 1901–1921.
Pachideh, V., Majdeddin Mir Mohammad Hosseini, S., 2019. A new physical model for studying flow direction and other influencing parameters on the internal erosion of soils. Geotech. Test. J. 42 (6), 1431–1456.
Palomino, A. M., Santamarina, J. C., 2005. Fabric map for kaolinite: Effects of pH and ionic concentration on behavior. Clays Clay Miner. 53 (3), 211–223.
Proia, R., Croce, P., Modoni, G., 2016. Experimental investigation of compacted sand-bentonite mixtures. Procedia Eng. 158, 51–56.
Rasheed, A., Dassanayake, S., Mousa, A., 2018. Suffusion susceptibility in gap-graded granular soils under variable hydraulic loading. In: 15th International Conference on Structural and Geotechnical.
Reichert, J. M., Norton, L. D., Favaretto, N., Huang, C., Blume, E., 2009. Settling velocity, aggregate stability, and interrill erodibility of soils varying in clay mineralogy. Soil Sci. Soc. Am. J. 73 (4), 1369–1377.
Rochim, A., Marot, D., Sibille, L., Thao Le, V., 2017. Effects of hydraulic loading history on suffusion susceptibility of cohesionless soils. J. Geotech. Geoenviron. Eng., 143 (7), 04017025.

Sutherland, B. R., Barrett, K. J., Gingras, M. K., 2015. Clay settling in fresh and salt water. Environ. Fluid Mech. 15 (1), 147–160.
Tsai, T. L., Chen, H. F., 2010. Effects of degree of saturation on shallow landslides triggered by rainfall. Environ. Earth Sci. 59 (6), 1285–1295.
Tu, S., Liu, X., Cai, H., 2022. Effect of gravity on colloidal particle transport in a saturated porous medium: Analytical solutions and experiments. PLoS One, 17 (10), 1–17.
Won, J., 2022. Assessment of internal stability of sand–fine mixture using particle detachment model and its implications on suffusion. Acta Geotech. 17 (10), 4667–4680.
Won, J., Choe, Y., Yang, Y., Choi, H., 2023. Impact of clay particle reattachment on suffusion of sand–clay mixtures. J. Rock Mech. Geotech. Eng. 15 (10), 2720-2730.
Won, J., Kim, T., Kang, M., Choe, Y., Choi, H., 2021. Kaolinite and illite colloid transport in saturated porous media. Colloid Surf. A-Physicochem. Eng. Asp. 626, 127052.
Xiong, H., Yin, Z. Y., Zhao, J., Yang, Y., 2021. Investigating the effect of flow direction on suffusion and its impacts on gap-graded granular soils. Acta Geotech. 16 (2), 399–419.
Xu, Z., Lin, P., Xing, H., Wang, J., 2021. Mathematical modelling of cumulative erosion ratio for suffusion in soils. Proc. Inst. Civ. Eng. Geotech. Eng. 174 (3), 241–251.
Zhang, L., Wu, F., Zhang, H., Zhang, L., Zhang, J., 2019. Influences of internal erosion on infiltration and slope stability. Bull. Eng. Geol. Environ. 78 (3), 1815–1827.
Zhang, Z., Liu, Z.D., Liu, G., et al., 2023. Prediction model of particle loss based on seepage tests of sediment in water-level-fluctuation zone of reservoir. Eng. Fail. Anal. 150, 107338.
Zhou, Z., Li, Z., Ranjith, P. G., Wen, Z., Shi, S., Wei, C., 2020. Numerical simulation of the influence of seepage direction on suffusion in granular soils. Arab. J. Geosci. 13 (14), 1–12.

Prof. Hangseok Choi attained a Bachelor of Engineering degree and a Master of Engineering degree at the Department of Civil Engineering of Korea University in Seoul, Korea, in 1993 and 1995, respectively. Subsequently, he received a Master of Science degree and a PhD with specialty of geotechnical and geo-environmental engineering at the Department of Civil and Environmental Engineering of the University of Illinois at Urbana-Champaign (UIUC) in 2000 and 2002, respectively. Prof. Choi was an assistant professor in Department of Civil Engineering of University of Akron, USA, from 2004 to 2005. He has been a professor in School of Civil, Environmental, and Architectural Engineering at Korea University since 2005. He is a vice president of ITA (International Tunnelling and Underground Space Association) and a vice president of KTA (Korean Tunnelling and Underground Space Association). In addition, he serves as a member of various Korean Government Advisory committees such as Major Infrastructure Design Council of Ministry of Land, Infrastructure and Transport, and Presidential Advisory Council for National Science and Technology. Prof. Choi has delivered a number of invited lectures and presentations and published more than 130 peer-reviewed international journal papers in the field of geotechnical engineering and tunnelling/underground space. He is currently serving as the senior editor of KSCE *Journal of Civil Engineering*.

HIGHLIGHTS

Paper title: Impact of flow direction on suffusion of sand-clay mixtures under variably saturated conditions

Authors: Yerim Yang, Yongjoon Choe, Jooho Lee, Jongmuk Won*, and Hangseok Choi*

- Soil column experiments tests were performed under variably saturated conditions.
- The impact of flow direction, clay type, and sand type on suffusion are discussed.
- Substantial suffusion was observed under downward flow for non-swelling clay.
- Reverse trend of suffusion between non-swelling and swelling clay was observed.
- Threshold size ratio where downward flow becomes more significant was proposed.

Declaration of interests

☒ The authors declare that they have no known competing financial interests or personal relationships that could have appeared to influence the work reported in this paper.

☐The authors declare the following financial interests/personal relationships which may be considered as potential competing interests: